APPLICATION OF THE H/V SPECTRAL RATIOS FOR EARTHQUAKE AND MICROTREMOR GROUND MOTIONS

Hiroshi KAWASE
DPRI, Kyoto University,
Gokasho UJI, Kyoto 611-0011
Japan

Francisco J. SÁNCHEZ-SESMA
Institute of Engineering,
Universidad Nacional Autónoma de México,
México

Shinichi MATSUSHIMA
DPRI, Kyoto University,
Gokasho UJI, Kyoto 611-0011
Japan

ABSTRACT

We propose an optimal way to use horizontal-to-vertical (*H/V*) spectral ratios for underground structure exploration, which is based on diffuse field concepts. This approach is applicable to earthquake and microtremor ground motions. For seismic motions we assume that a set of incoming elastic plane waves with various azimuths, incidences, and polarizations will form a spatially homogeneous wavefield. For microtremors we assume that randomly distributed sources, mostly close to the surface, will generate them. In both cases the motions are considered as belonging to multiple scattered diffuse fields. Then the stack of normalized Fourier transformed autocorrelation functions, that is, the average of spectral densities should correspond to the imaginary part of the Green's function. For seismic motions we demonstrated that this imaginary part of the Green's function is proportional to the square of the absolute value of the one-dimensional (1D) transfer function for normal incidence. We first compared averaged synthetics of 1D underground structure with the prediction for *H/V*. After summing up hundreds of plane wave synthetics, we obtained *H/V* ratios that converge to the theoretical prediction. We show examples for observed data at two K-NET stations in Japan. We found that earthquake *H/V* ratios are quite stable from earthquake to earthquake. Besides, they exhibit obvious differences from *H/V* ratios of microtremors. This fact may provide us a double constraint to inversion coming from different theoretical treatments.

INTRODUCTION

When seismic motion is dominated by multiple scattering of waves, its energy densities have a diffusion-like behavior. In reality, these scattering waves sample the medium along their multiple paths. Diffusion-like regimes are obtained when the field is engendered by equipartitioned illumination. This is usually attributed to multiple scattering because equipartition can be achieved by a distributed uniform set of random forces (e.g. Sánchez-Sesma *et al.* 2008). Under these conditions, the Green's function retrieval (GFR) stems from averaging cross correlations of the recorded motions of such diffuse field (e.g. Campillo and Paul, 2003; Weaver and Lobkis, 2001; Wapenaar, 2004; Chávez-García and Luzón, 2005; Sánchez-Sesma and Campillo, 2006; Gouédard *et al.*, 2008; Yokoi and Margaryan, 2008; Sato, 2010). This interferometry approach has been used to retrieve surface wave characteristics as they are the most prominent part of the Green's functions.

In this study we consider strong ground motion in elastic layered media. We explore the theoretical consequences of assuming both a "sufficiently" flat layered site and various earthquake sources that are "sufficiently" deep, in such a way that surface waves are not dominant or do not appear yet in the target windows. In fact, surface waves may carry most of the effects of lateral heterogeneity and they have certainly a three dimensional (3D) nature. In this way we strictly enforce the one dimensional (1D) wave propagation, neglecting surface waves. Thus, average autocorrelations can be related to the imaginary part of the 1D Green's function, when the source and receiver are both at the same point.

For 1D layered media Claerbout (1968) discovered the relationship between reflection response and autocorrelation of surface motion. As an extension of Claerbout's (1968) result, we show that the imaginary part of the 1D Green's function at the surface for a surface source is equal to the square of the absolute value of the transfer function for an incoming unit displacement divided by four times the

circular frequency and the half-space (bedrock) impedance. We explore the connection of this result with the illumination due to earthquakes in order to construct new formulations for the average horizontal-to-vertical (*H/V*) spectral ratio of earthquake motions. To model the diffuse wave field we assume a set of incoming plane waves (of P, SV, and SH types) with varying azimuths, incidence, and polarization angles covering the space and consider a layered medium. The final result is a very simple formula where we can easily calculate theoretical *H/V* ratios based on simple transfer functions due to the vertical incidence of body waves in a 1D medium.

The use of *H/V* spectral ratios of earthquake motions, as well as microtremors, has been discussed for a long time. Bard (1999) provided an extensive review of studies on microtremors starting from the observational studies of Kanai and his group in Japan as early as the 1950s. In fact the microtremor *H/V* spectral ratio has been the subject of considerable numbers of studies to clarify its strengths and limitations (e.g., Nakamura, 1989; Lachet and Bard, 1994; Mucciarelli, 1998, and Mucciarelli and Gallipoli 2001; Arai and Tokimatsu, 2004; Bard, 2008; Pilz *et al.*, 2009). Also the use of *H/V* ratios for microtremor was one of the primary topics during the last ESG symposium in Grenoble, France in 2006. However, until recently, the search for a theoretical solution for the *H/V* ratio of microtremors has been so far futile.

Under the assumption that the seismic field is a diffuse one, it has been recently proposed that the *H/V* ratio for microtremors recorded at a receiver on the surface of a horizontally layered medium can be computed in terms of the imaginary part of the Green's function at the receiver (Sánchez-Sesma *et al.*, 2011). It links average energy densities with the Green's function in 3D. The theory allows us computing the *H/V* ratio as an intrinsic property of the medium. When dealing with microtremors, the Green's function implies that the loaded and observation points must be the same. This strongly suggests that surface waves play an important role in the evaluation of *H/V* ratios, although we do not need to assume that microtremors consist only of surface waves as in most of the previous studies.

For earthquake motions, in the 1980s the time-domain *R/V* ratio technique, that is, the so-called "receiver function method" was established for the long period earthquake motions at teleseismic distances. As for studies on relatively higher frequency (and hence for shallower layers), Lermo and Chávez-García (1993) applied the *H/V* ratio technique for earthquake motions, probably for the first time. Satoh *et al.* (2001) presented a review of relevant papers including those for S coda. However, these studies are all considered to be a deterministic approach of the *H/V* ratios, apart from the approach presented herein. In the next section we will briefly explain the derivation procedure of the theoretical *H/V* ratio, the detail of which can be found in Kawase *et al.* (2011).

RESPONSE OF A 1D MEDIUM SUBJECTED TO BODY WAVES ONLY

For most earthquakes, the local structure around the observation site will be illuminated mainly by plane body waves from the source with multiple reflections and refractions, so that ground motions are composed essentially of plane waves. If our medium has depth-dependent (i.e., 1D) properties, it is reasonable to assume statistical equivalence in the horizontal directions. As a consequence, we describe the problem as 1D and so from the diffuse field concept (Sánchez-Sesma *et al.*, 2008) we can write:

$$\left\langle H^2 \right\rangle \propto \mathrm{Im}[G_{11}^{1D}(0,0;\omega)] + \mathrm{Im}[G_{22}^{1D}(0,0;\omega)], \quad \text{and}$$

$$\left\langle V^2 \right\rangle \propto \mathrm{Im}[G_{33}^{1D}(0,0;\omega)], \tag{1}$$

where $\left\langle H^2 \right\rangle$, and $\left\langle V^2 \right\rangle$ are the averages of the horizontal and vertical autocorrelations, respectively, and $G_{ij}^{1D}(\mathbf{x},\mathbf{y};\omega)$ is the Green's function of the 1D structure at the circular frequency ω. It is common practice to eliminate the angular brackets while writing the expression for the average *H/V* spectral ratio to have:

$$\frac{H(\omega)}{V(\omega)} = \sqrt{\frac{\mathrm{Im}[G_{11}^{1D}(0,0;\omega)] + \mathrm{Im}[G_{22}^{1D}(0,0;\omega)]}{\mathrm{Im}[G_{33}^{1D}(0,0;\omega)]}}, \tag{2}$$

This fundamental formula is a direct consequence of the diffuse wave theory for GFR, when the two observation points coincide (i.e., autocorrelation is taken). For a horizontally homogenous medium $G_{11}^{1D}(\mathbf{x},\mathbf{x};\omega) = G_{22}^{1D}(\mathbf{x},\mathbf{x};\omega)$ and we can write

$$\frac{H(\omega)}{V(\omega)} = \sqrt{\frac{2\operatorname{Im}[G_{11}^{1D}(0,0;\omega)]}{\operatorname{Im}[G_{33}^{1D}(0,0;\omega)]}} \ . \tag{3}$$

Nakahara (2006a) studied systematically the relationships between the spatial correlations and the Green's functions in 1D, 2D and 3D in random scalar fields. Here, we deal only with the 1D wavefield, which is analogous to the elastic case when we consider only vertically propagating plane waves. In the elastic case the horizontal and vertical motions are due to shear (S) and compressional (P) waves, respectively, but no coupling between them is necessary to be considered here, since they are restricted to be vertically propagating waves.

When we derive wave propagation equations within a stack of 1D layers following Aki and Richards (1980), we obtain

$$\operatorname{Im}[G(0,0;\omega)] = (4\omega\rho_H c_H)^{-1}|TF(\omega)|^2 \ . \tag{4}$$

This result holds for the 1D elastic case where c is substituted with α or β in the case of P or S waves, respectively. Displacements will then be vertical or horizontal corresponding to each case. This result is implicit both in Claerbout's (1968) and Nakahara's (2006b) developments. However, to the best of our knowledge the relationship between the imaginary part of the 1D Green's function at the surface of a surface source and the transfer function for an incoming unit wave from a half space has not been pointed out before Kawase *et al.* (2011).

Consider Equation 3 and specialize Equation 4 for both horizontal and vertical motions, that is, derive a transfer function for the horizontal motion due to S wave, $TF_1(\omega)$, and the other one for the vertical motion due to P wave, $TF_3(\omega)$. We may write a simple formula for an *H/V* spectral ratio on the surface as:

$$\frac{H(0,\omega)}{V(0,\omega)} = \sqrt{\frac{2\alpha_H}{\beta_H}}\frac{|TF_1(0,\omega)|}{|TF_3(0,\omega)|}, \tag{5}$$

where we added zero inside the parenthesis to represent the depth of the source and receiver at the surface. It can be shown that at the bottom of the layering, at $z = h$, the following similar formula holds:

$$\frac{H(h,\omega)}{V(h,\omega)} = \sqrt{\frac{2\alpha_H}{\beta_H}}\frac{|TF_1(h,\omega)|}{|TF_3(h,\omega)|} \ . \tag{6}$$

This equation can be used for the inversion of a layered structure from borehole records of receivers embedded inside such a layered structure. From these equations it is clear that we can also retrieve P to S wave velocity ratios of the bedrock from the observed *H/V* ratios, since the low-frequency asymptote of the transfer function ratio should be one.

NUMERICAL COMPUTATIONS

To provide a numerical validation of the simple theory, we first generate a series of synthetics as the pseudo-random white noise time--histories with cosine-shaped windows on both sides. We produce synthetics for a 1D layered structure with specific incidence, azimuth, and polarization angles of S and P waves that may cover their realistic ranges of values.

Table 1. Assumed structure as MYG014 model, whose S wave velocities are taken from those of MYG014 obtained from boring exploration up to 20 meters by NIED and inverted by Kawase and Matsuo (2004) and Kawase (2006) below 20 meters.

| No.	density ρ (g/cm	damping h	Thickness (m)	S wave velocity β (m/s)	P wave velocity α (m/s)
1	1.61	0.011	0.40	130	400
2	1.61	0.011	1.30	130	400
3	1.61	0.011	0.30	130	400
4	1.89	0.011	1.70	310	1500
5	1.89	0.011	0.30	310	1500
6	1.70	0.011	3.35	200	1250
7	1.70	0.011	0.65	200	1250
8	2.00	0.011	22.45	560	2200
9	2.28	0.011	70.00	1732	3500
10	2.47	0.011	80.00	2253	4500
11	2.56	0.011	120.00	3010	5200
12	2.67	0.011	∞	3400	5888

Fig.1. Comparison of the H/V ratio calculated as the average spectral ratio of the generated synthetics with 300(S)+60(P) realizations for different incident and azimuth angles for MYG014 model (gray line) with the theoretical one calculated by using Equation 5 (broken line).

In this synthetic simulation we rigorously calculate the elastic wave propagation phenomena in a layered half space based on the transmission-reflection coefficient method (Aki and Richards, 1980) with inclined incidence of S and P waves so that mode conversions between them at all the interfaces of layers and the surface are taking into consideration. SH and SV wave amplitudes are determined as directional cosines in the horizontal and vertical directions, respectively, for the assumed polarization angle of S waves so that the energy is distributed equally on the average. As a reference case, we use 60 synthetics for P and S wave incidence (five different incidence angles and twelve different azimuth angles), and we consider five different polarization cases for S wave so that we actually generate 300 synthetics for the S wave components and 60 synthetics for the P wave component. In this simple scheme, the average energy of S waves is considered to be five times that of P waves as this is the ratio of the number of incidences for S and P waves.

The velocity structures used here correspond to the two models shown in Tables 1. This model has eleven layers whose velocities are set as the velocities at the MYG014 K-NET site (See Kinoshita, 1998 for K-NET information). For the upper eight layers, we used P-S logging information provided by NIED. For the lower three layers we used S wave velocities inverted in order to reproduce the S wave site factor derived from the Spectral Inversion Technique (Kawase and Matsuo, 2004; Kawase, 2006). The P wave velocities are assumed based on the corresponding S wave velocities. The half-space below is assumed to have the S wave velocity of β = 3,400m/s as in Kawase and Matsuo (2004). We also assume 1.1 % of frequency-independent damping h, which is equivalent to Q=45.

Figure 1 shows the comparison of the synthetic *H/V* ratio and the theoretical one calculated by using Equation 5 for the MYG014 model. The *H/V* ratios are almost identical, although synthetics have small fluctuations around the theoretical one. This figure proves that calculating the summation of power spectral densities or the Fourier transform of the autocorrelation function of earthquake motions on the surface and taking their *H/V* ratios really yields the theoretical *H/V* ratio, namely, the transfer function ratio between the S and P wave incidences with a correction coefficient as a function of the velocity ratio between P and S waves of the bedrock, which is 1.86 for a Poisson solid.
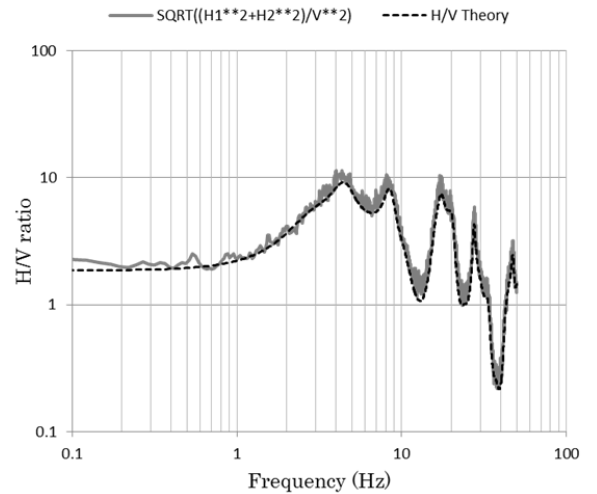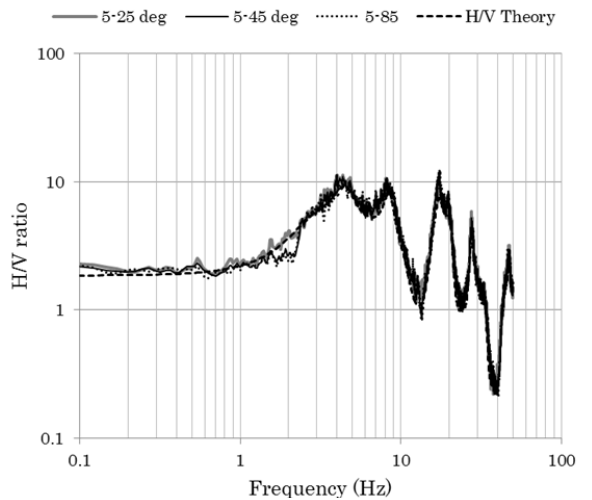

Fig.2. Comparison of the H/V ratios calculated as the average spectral ratios of the generated synthetics for MYG014 model with incidence angles in the ranges i) between 5° to 25° as in Fig.1, ii) 5° to 45°, and iii) 5° to 85°. The numbers of synthetics are 300 (S) and 60 (P) for all the cases. The theoretical ratio calculated by using Equation 5 is also shown (broken line).

Figure 2 shows comparisons of different ranges of incident angles. As the reference case shown so far, we choose the range of incidence angle from 5° to 25°, by considering realistic situation for direct body wave from sources close to the site. We add two test cases, one of which covers the range from 5° to 45° and the other from 5° to 85°. The number of synthetics is the same as that in the reference case, namely, 300 for S wave and 60 for P wave, and MYG014 model is used. We can see a few conspicuous troughs for cases in which the range of the incidence angle is large. This must come from the theoretical extraordinary phenomenon due to super-critical incidence of SV wave, and hence we could never actually observe.

Thus numerical examinations reveal that our proposed formulation is valid for *H/V* spectral ratios of a layered half space. In the final form of our average formulations, Equations 5 and 6, we completely exclude mode conversions in body waves, while they occur in each of the individual realizations with diverse incident angles in our numerical examination. Our average spectral densities for synthetics surprisingly cancel out the effects of such conversions and converge rapidly to the values predicted by our average formulation. This makes the proposed theory remarkable and valuable for practical application.
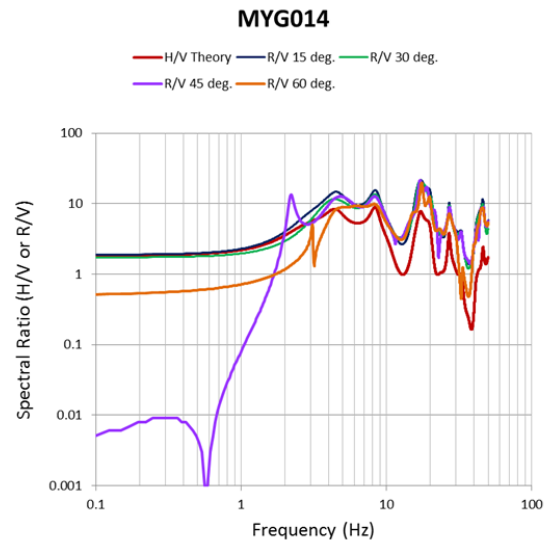

Fig.3. Comparison of the H/V ratio for MYG014 model by using Equation 5 (red line) with the theoretical R/V ratios calculated for single SV wave incidence (other lines for different incidence angles).

DETERMINISTIC INCLINED SV WAVE INCIDENCE (*R/V* RATIO)

As mentioned in Introduction we have been using theoretical ratios of radial component with respect to the vertical component, the so-called *R/V* ratios and interpret it as the result of SV wave mode conversion for a long time. In this theory it is assumed to have SV wave incidence only in a coherent manner, which is totally opposite assumption of ours. It is interesting to compare theoretical *H/V* ratios in the diffuse concept to the *R/V* ratios for an incident SV wave.

Figure 3 compares our theoretical *H/V* ratios with the *R/V* ratios for a single realization of an inclined SV wave incidence. As we can see the *R/V* ratios below the critical angle (θ=15° and 30°) seems quite similar to the theoretical *H/V* ratios, although amplitude of the *H/V* ratio is smaller in the higher frequency range. For super-critical incidences low-frequency ratios are quite different from that of *H/V* ratios, however, high frequency characteristics are still quite similar to each other. This comparison suggests that interpretation of earthquake *H/V* ratios in a diffuse regime by using *R/V* ratio of a single realization of SV wave incidence could be a viable solution, especially by assuming sub-critical incidences. This explains why we have been using *R/V* interpretation for such a long time. However, if we use the theoretical *H/V* ratios proposed here, then we can rely on the amplitude as well.

OBSERVED *H/V* RATIOS OF EARTHQUAKE MOTIONS AT MYG014

We present here examples of the proposed method applied to actual earthquake ground motions observed at the K-NET sites in Japan (Kinoshita, 1998). Figure 4 shows the square root of NS, EW, and UD components' power spectral densities averaged over thirteen earthquake ground motions observed at MYG014. No normalization is applied for each earthquake. As a simple rule for excluding records with strong nonlinearity effects on *H/V* ratios, throughout the study, we use only those records with Peak Ground Acceleration (PGA) less than 200 cm/s^2. We can see quite similar values for the NS and EW components, while for the UD component it is significantly deficient between 2 to 6 Hz.

Because of this difference, the *H/V* ratio at MYG014 in Figure 5 shows clear amplification in that frequency range, the level of which reaches one order of magnitude. In the higher frequency range, we can still see peaks and troughs with amplitudes of around 5 or 0.5. In this figure we also show the theoretical *H/V* ratio, shown in Figure 1, calculated by using the velocity structure of MYG014 model (Table 1). Although there is a noticeable
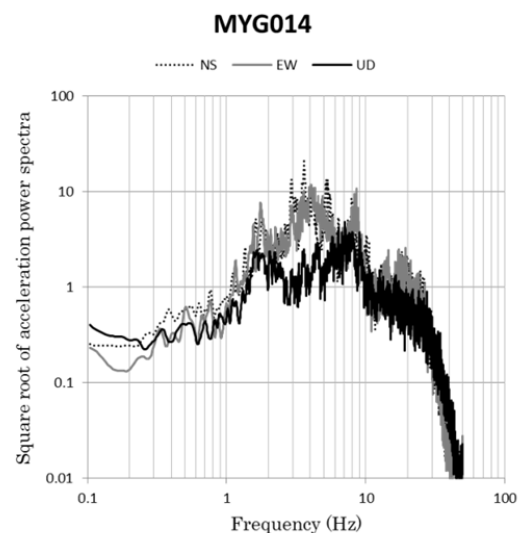

Fig.4. Square root of the power spectral densities of the three components averaged over thirteen earthquake ground motions observed at MYG014. No normalization is applied.

difference in the trough amplitude at around 7 Hz, peak-out frequencies of major peaks and troughs as well as overall spectral characteristics are quite similar to each other. We should note that the trough at around 40 Hz in the observed *H/V* ratio has amplitude less than 1, which is much less than the *R/V* ratios for sub-critical incidence as seen in Figure 3.

As the basic concept for theoretical derivation of Equation 5 we assume that the incident waves to a 1D layered structure consist purely of body waves, either direct or scattered, without any surface wave contributions. For practical application we need to check if this technique is applicable in any part of the observed seismic motions. Figure 6 shows comparison of *H/V* ratios at MYG014 for the P wave part from the onset of P wave till the onset of S wave, the S wave part of 10 s in duration, and the coda part of 30 s in duration from twice the P-to-S time after the onset of S wave in comparison to the *H/V* ratio for the whole duration, which is varying from earthquake to earthquake but typically around 70 to 120 s. We can see that the S wave part and the coda part yield quite similar *H/V* results to that of the whole duration. However, the P wave part shows smaller *H/V* ratios than the others from 0.3Hz to 30Hz. This is probably due to insufficient generation of horizontally polarized S wave caused by scattering and reflection/refraction for P wave incidence within the short P-to-S time. Note that the conspicuous trough at 40 Hz exists for all the time segments, which means that this trough should be created by the P wave (i.e., vertical component) peak at the site.

OBSERVED *H/V* RATIOS OF EARTHQUAKE MOTIONS AT MYG004

Finally we would like to see another K-NET site, MYG004 at Tsukidate, where we have the world record of the horizontal peak ground acceleration (HPGA) of 2.7 g during the Off Pacific Coast, Tohoku, Japan earthquake of March, 11, 2011 (K-NET site; http://www.k-net.bosai.go.jp/k-net/topics/TohokuTaiheiyo_ 20110311/ nied_kyoshin2e.pdf). This site is located in the northern part of the Miyagi Prefecture, 50km north of the Sendai City along the river plain of the Hasama River, a branch of the major Kitakami River. Figure 7 shows Google Satellite Image around the MYG004 site. As we can see the station is rested on the flat flank of a small hill as shown in Figure 8. We inevitably have a topographic effect as well as a soil amplification effect due to this small hill.

At MYG004 the boring data shows that we have only a 1m of surficial clay layer on top of the rock formation, although top 9m of this rock formation seem strongly weathered. Table 2 shows the assumed structure whose S wave velocities are taken from those of MYG004 obtained from boring exploration up to 10 meters by NIED and inverted by Kawase and Matsuo (2004) and Kawase (2006) below 10 meters. As we can see later the inverted structure for this site does not perform so well.

Before the Tohoku earthquake of 2011 Kawase and Matsuo (2004) and Kawase (2006) used the so-called generalized inversion technique to separate source and path effects from a lot of observed spectra for observed data of K-NET, KiK-net, and JMA Shindokei network to obtain site effects at all the sites where we have more than three earthquakes. Figure 9 shows horizontal and vertical components' site amplification factors relative to the horizontal component at the reference station, YMGH01, where we have the bedrock S wave velocity of 3,400 m/s. As we can see significant amplification exists in the low frequency as low as 1Hz and 20 times at around 10Hz in the horizontal component. For vertical component amplification is much less, around 2 to 4.
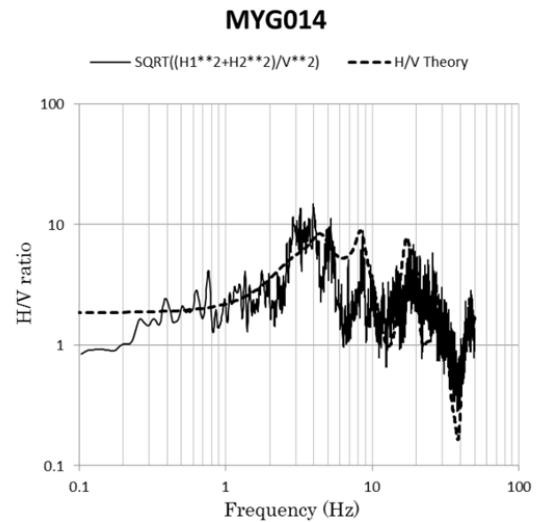

Fig.5. H/V ratio calculated as the average spectral ratios of observed three components at MYG014 shown in Fig.4 (solid line), together with the 1D theoretical prediction calculated for MYG014 model shown in Fig.1 (broken line). Parzen window of 0.05 Hz is applied for the observed spectra hereafter for the whole duration of the data.
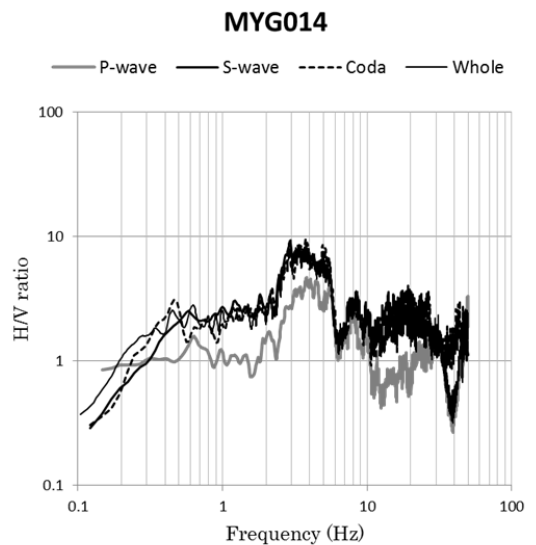

Fig.6. Comparison of H/V ratios at MYG014 for i) P wave part from the onset of P wave till the onset of S wave, ii) S wave part with a duration of 10 s, iii) coda part with a duration of 30 s starting from twice the P-to-S time after the onset of S wave, and iv) the whole duration, the length of which varies for each earthquake (typically from 70 to 120 s). Normalization with respect to the total energy is applied. In order to smooth the spectra Parzen window of 0.1 Hz is used for P wave part, S wave part, and coda part.

Fig.7. *Google satellite image around MYG004 K-NET site. It is close to the Kurihara City Hall.*

Fig.8. *Photo of the small hill on which MYG004 K-NET site is situated. The direction of photo is from north northwest to south southeast. The flat part in front of the site is the parking lot of the Kurihara Cultural Hall (Bunka-Kaikan).*

As we have proved that as long as *H/V* spectral ratios are our primary concern, we do not need to separate site effects for two components at a site, but just we need to take the average of all the spectra for two horizontal components and one vertical component and then take the ratio as Equation 5. In Figure 10 we compares *H/V* ratio obtained as such for earthquakes occurred during the period from August, 1996 to May 2002 (the same period of Kawase and Matsuo, 2004) with the *H/V* ratio calculated from the separated site factors shown in Figure 9. The correspondence is basically good for these two observed *H/V* ratios. The black dotted line in Figure 10 shows the 1D theoretical *H/V* ratio by using the information summarized in Table 2, which overestimates the highest peak at 10Hz and yields the fundamental peak frequency (~3.5Hz) lower than the observed (~5Hz).

Table 2. *Assumed structure as MYG004 model, whose S wave velocities are taken from those of MYG004 obtained from boring exploration up to 10 meters by NIED and inverted by Kawase and Matsuo (2004) and Kawase (2006) below 10 meters.*

No.	density ρ (g/cm³)	damping h	Thickness (m)	S wave velocity β (m/s)	P wave velocity α (m/s)
1	1.64	0.011	1.00	100	280
2	1.96	0.011	0.20	240	940
3	1.96	0.011	2.80	240	940
4	1.99	0.011	6.25	550	1800
5	2.18	0.011	20.00	1364	2729
6	2.37	0.011	110.00	2075	3594
7	2.54	0.011	50.00	2874	4978
8	2.67	0.011	∞	3400	5888

After the main shock of the Tohoku earthquake of 2011, we have plenty of aftershock data at all the stations in the epicentral region. At MYG004 we use 53 earthquakes observed from March 9, 2011 to May, 17, 2011, excluding the main shock and the aftershock of April, 7 with the second largest PGA. Figure 11 shows all the *NS/V* and *EW/V* ratios for 53 earthquakes and their average ratio together with average ± one standard deviation for the whole duration. We can see large fluctuations from earthquake to earthquake but on the average we have common characteristics. The peak amplitudes at 1 Hz, 4 Hz, and 10Hz are all similar to the one for earthquakes well before the main shock, although troughs in the high frequency range have sharper shapes than the one shown in Figure 10.

As for the main shock and the largest PGA aftershock the *H/V* ratios are noticeably different from the weak motions, as shown in Figure 12. This is clearly a manifestation of soil nonlinearity. The predominant peak at 10Hz is systematically moving toward the lower frequency side down to 4 Hz for the main shock. We will investigate in more detailed manner the pervasive nonlinear site effect emergence in the main shock and large aftershock records in future.
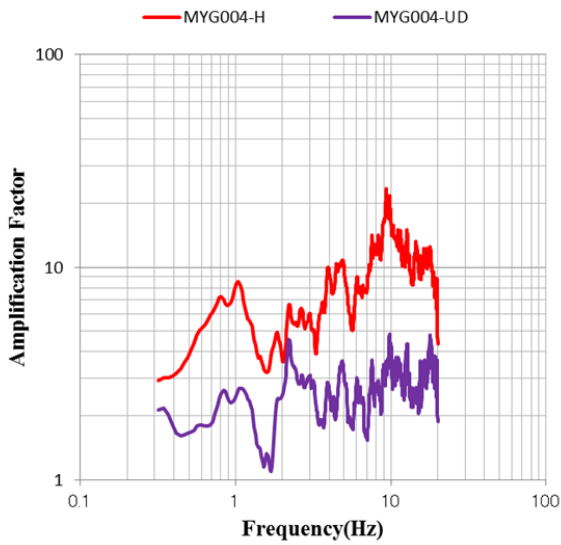
Fig.9. Site amplification factors of horizontal and vertical components relative to the horizontal component at the reference station, YMGH01, where we have the bedrock S wave velocity of 3,400 m/s. Analysis is done from 0.3 Hz to 20 Hz using only the S wave part (Kawase & Matsuo, 2004).
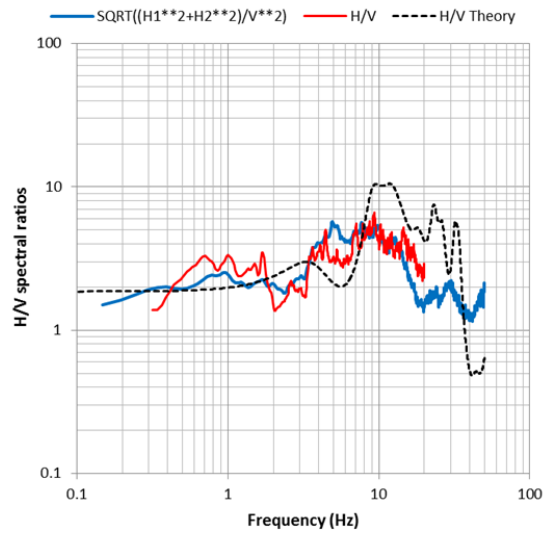

Fig.10. Comparison of H/V ratio obtained by Equation 5 for only S wave part of 10 seconds with the one calculated from the separated site factors shown in Fig.9 at MYG004. The black dotted line shows the 1D theoretical H/V ratio from the information summarized in Table 2.
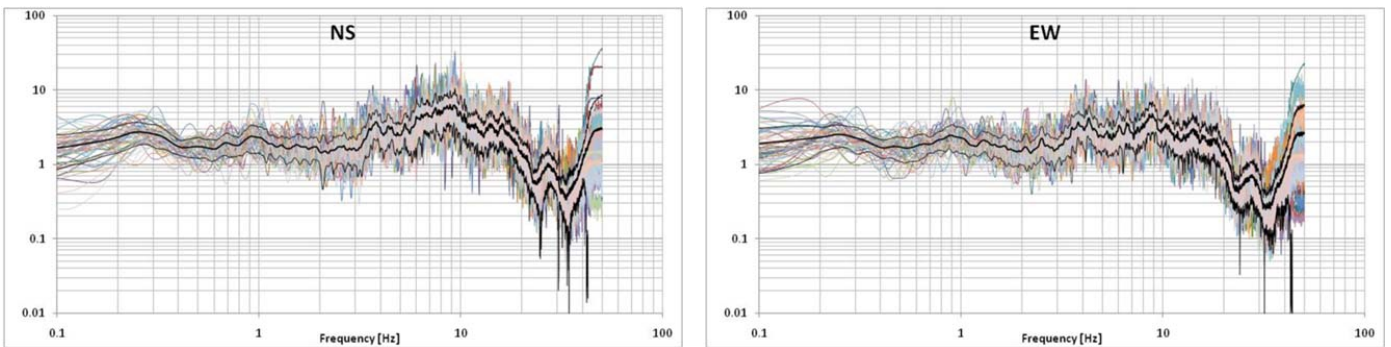

Fig.11. NS/V and EW/V spectral ratios for 53 earthquakes and their average ratio together with average ± one standard deviation. The whole duration of the observed accelerograms are used.
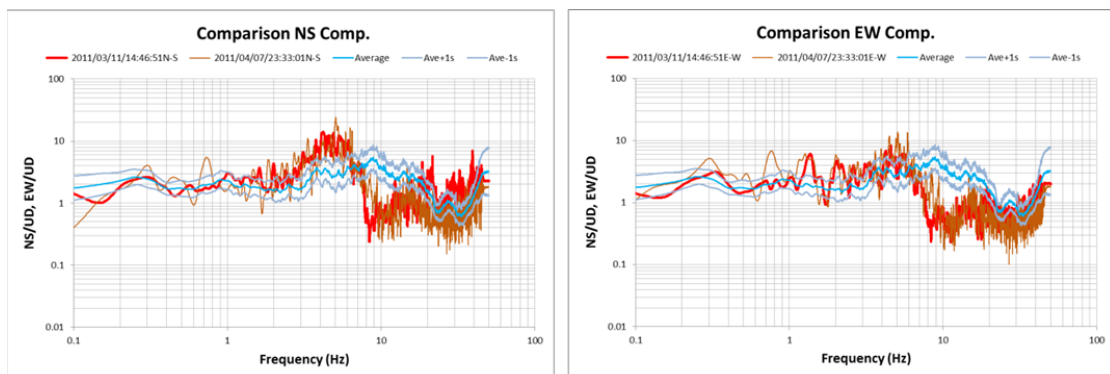

Fig.12. NS/V and EW/V spectral ratios for the main shock and the largest PGA aftershock in comparison to the average H/V ratios of two horizontal components for weak (<200 Gals) motions. The whole duration of the observed accelerograms are used.

H/V RATIOS OF EARTHQUAKE MOTIONS AND MICROTREMORS AT MYG004

Finally we compare *H/V* ratios at MYG004 for microtremors and earthquakes. Fig. 13 shows comparisons of *NS/V* and *EW/V* spectral ratios of microtremors at the site observed in April 29, 2011 with the average and average ± one standard deviation *H/V* ratios of the 53 foreshocks and aftershocks (two components are mixed to calculate average). Overall characteristics are quite similar to each other, however, details of their behavior are somewhat different. For example highest peak frequency is higher in microtremors at around 25 Hz than earthquakes, while after the deep trough amplitude is coming back in earthquakes, not in microtremors as the frequency goes higher. These differences should come from the difference of dominant diffuse wave fields in earthquakes and microtremors and therefore different theoretical treatment may lead to more stable inversion for a velocity structure around the site.
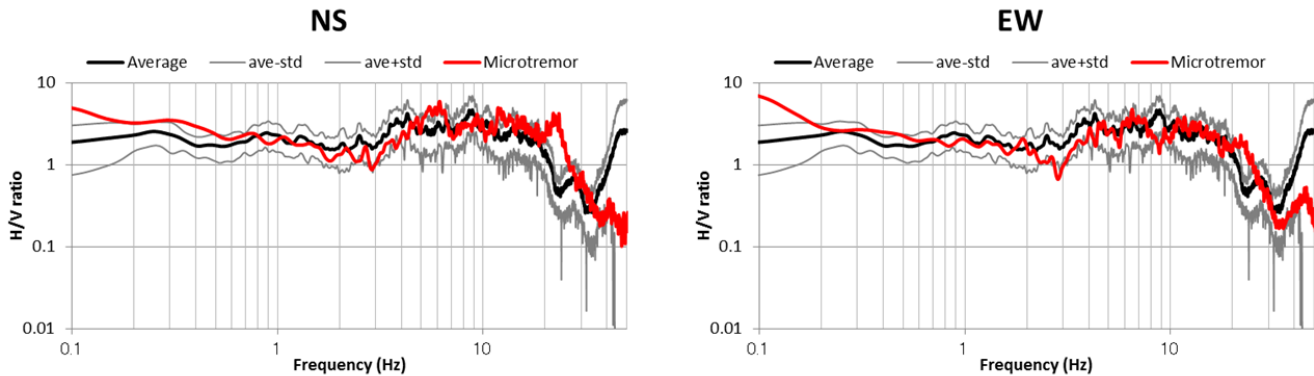

Fig.13. NS/V andEW/V spectral ratios for the microtremors in comparison to the average H/V ratios of two horizontal components for earthquake weak (<200 Gals) motions. Only microtremors we use NS/V and EW/V ratios.

CONCLUSIONS

We have derived first theoretical formulation for *H/V* of earthquakes where the major contribution of seismic energy assumed to be of body wave types coming from a deeper part of the earth as diffuse wave field. From the correspondence of autocorrelation function to the imaginary part of the Green's function for the source collocated with the receiver and the Claerbout's formula between 1D transfer function and the imaginary part of the Green's function, we can derive a simple formula to calculate *H/V* ratios for any 1D structure in case of earthquake ground motions. We have proved by using synthetics that this theory really works for the mixture of different S and P waves incident to 1D structure with various angles of incidence, azimuth, and polarization. The conventional *R/V* ratios will give similar values of our theoretical *H/V* ratios as long as the incidence angle is less than the critical one.

When we applied the theory to the actual ground motions, we can see quite a nice match if we have a good 1D structure. In the case of a 2D/3D structure around a site we may need to use 2D/3D Green's functions for body waves. Yet the diffuse wave field theory holds as long as we have sufficient duration of seismic motion to have sufficiently random scattering. We found that the earthquake *H/V* ratios are quite stable for most of the cases, except for very severe level of input. Further study will be necessary for 2D/3D effects on *H/V* ratios, as well as soil nonlinearity for a large input as we can see in the case of the main shock of the Tohoku earthquake of March 11, 2011.

We have compared *H/V* ratios for earthquakes with microtremors just to see how similar or dissimilar to each other. They are similar in general but dissimilar in their details. Since our formulation of *H/V* for microtremors (Sánchez-Sesma *et al.*, 2011) and earthquakes (Kawase *et al.*, 2011) are different because of the different loading features, and so they will provide double constraints for the inversion of velocity structure around a site. After successful inversion of the velocity structure around a site we can calculate site amplifications for any types of incident waves, either body or surface waves.

As mentioned in Introduction it has been discussed for a long time about the physical reality of the H/V ratios and their theoretical correspondence for seismic motions and micorotremors. After the advent of the diffuse wavefield theory for seismic motions (Kawase *et al.*, 2011) and microtremors (Sánchez-Sesma *et al.*, 2011), we need no longer to use Rayleigh wave ellipticity nor R/V ratios of unknown angles of SV wave incidence to interpret observed H/V ratios, as long as the duration of observation or number of records is sufficient to assume the establishment of disuse wavefield. This clarification on the theoretical entity of the H/V ratios may have strong impact to the practical use of H/V ratios for site classification in earthquake engineering and applied seismology.

REFERENCES

Aki, K. and P.G. Richards [1980], "*Quantitative Seismology. Theory and Methods*", W. H. Freeman, San Francisco.

Arai, H. and K. Tokimatsu [2004], "S-Wave Velocity Profiling By Inversion of Microtremor H/V Spectrum", *Bull. Seism. Soc. Am.* **94**, 53–63.

Bard, P.-Y. [1999], "Microtremor Measurement: A Tool for Site Effect Estimation?", *Proc. 2nd International Symposium on the Effect of Surface Geology on Seismic Motion*, Yokohama, Japan, 1251–1279.

Bard, P.-Y. [2008], "The H/V Technique: Capabilities and Limitations Based on the Results of the SESAME Project", Foreword, *Bull. Earthq. Eng.,* **6**, 1–2 DOI 10.1007/s10518-008-9059-4.

Campillo, M. and A. Paul [2003], "Long Range Correlations in the Seismic Coda", *Science,* **299**, 547-549.

Chávez-García, F.J. and F. Luzón [2005], "On the Correlation of Seismic Microtremors", *J. Geophys. Res.,* **110**, B11313, doi:10.1029/2005JB003671.

Claerbout, J.F. [1968], "Synthesis of a Layered Medium from Its Acoustic Transmission Response", *Geophysics* **33**, 264-269.

Gouédard, P., L. Stehly, F. Brenguier, M. Campillo, Y. Colin de Verdiére, E. Larose, L. Margerin, P. Roux, F.J. Sánchez-Sesma, N.M. Shapiro, and R.L. Weaver [2008], "Cross-Correlation of Random Fields: Mathematical Approach and Applications", *Geophys. Prospecting,* **56**, 375-393.

Kawase, H. and H. Matsuo [2004], "Amplification Characteristics of K-NET, Kik-NET, and JMA Shindokei Network Sites Based on the Spectral Inversion Technique", *13th World Conference on Earthquake Engineering*, Vancouver, Canada, Paper No. 454.

Kawase, H. [2006], "Site Effects Derived From Spectral Inversion Method for K-NET, Kik-Net, and JMA Strong-Motion Network with Special Reference to Soil Nonlinearity in High PGA Records", *Bull. Earthq. Res. Inst., Univ. Tokyo,* **81**, 309-315.

Kawase, H., F. J. Sánchez-Sesma, and S. Matsushima [2011], "The Optimal Use of Horizontal-To-Vertical Spectral Ratios of Earthquake Motions for Velocity Inversions Based on Diffuse Field Theory for Plane Waves", *Bull. Seism. Soc. Am.,* **101** (in press).

Kinoshita, S. [1998], "Kyoshin Net (K-Net)", *Seism. Res. Lett.* **69**, 309–334.

Lermo, J. and F.J. Chávez-García [1993], "Site Effects Evaluation Using Spectral Ratios with Only One Station", *Bull. Seism. Soc. Am.* **83**, 1574-1594.

Lachet, C. and P.-Y. Bard [1994], "Numerical and Theoretical Investigations on the Possibilities and Limitations of the "Nakamura's" Technique", *Journal of Physics of the Earth,* **42**, 377-397.

Mucciarelli, M. [1998], "Reliability and Applicability of Nakamura's Technique Using Microtremors: An Experimental Approach", *Journal of Earthquake Eng.,* **2**, 1-14.

Mucciarelli, M. and M.R. Gallipoli [2001], "A Critical Review of 10 Years of Microtremor HVSR Technique", *Bollettino di Geofisica Teorica ed Applicata,* **42**, 255-266.

Nakahara, H. [2006a], "A Systematic Study of Theoretical Relations Between Spatial Correlation and Green's Function in One-, Two- and Three-Dimensional Random Scalar Wavefields", *Geophys. J. Int.,* **167**, 1097–1105 doi: 10.1111/j.1365-246X.2006.03170.x

Nakahara, H. [2006b], "Theoretical Background of Retrieving Green's Function by Cross-Correlation: One-Dimensional Case", *Geophys. J. Int.,* **165**, 719-728 doi: 10.1111/j.1365-246X.2006.02916.x

Nakamura, Y. [1989], "A Method for Dynamic Characteristics Estimation of Subsurface Using Microtremor on the Ground Surface", *Quaterly Report Railway Tech. Res. Inst.*, **30**, 25-30.

Pilz, M., S. Parolai, F. Leyton, J. Campos, and J. Zschau [2009], "A Comparison of Site Response Techniques Using Earthquake Data and Ambient Seismic Noise Analysis in the Large Urban Areas of Santiago de Chile", *Geophys. J. Int.,* **178**, 2, 713-728.

Sánchez-Sesma, F. J. and M. Campillo [2006], "Retrieval of the Green's Function from Cross-Correlation: The Canonical Elastic Problem", *Bull. Seism. Soc. Am.,* **96**, 1182-1191.

Sánchez-Sesma, F.J., J.A Pérez-Ruiz, F. Luzón, M. Campillo, and A. Rodríguez-Castellanos [2008], "Diffuse Fields in Dynamic Elasticity", *Wave Motion,* **45**, 641–654.

Sánchez-Sesma, F.J., M. Rodríguez, U. Iturrarán-Viveros, F. Luzón, M. Campillo, L. Margerin, A. García-Jerez, M. Suarez, M.A. Santoyo, and A. Rodríguez-Castellanos [2011], "A Theory for Microtremor *H/V* Spectral Ratio: Application for a Layered Medium", *Geophys. J. Int.* (In Press).

Sato, H. [2010], "Retrieval of Green's Function Having Coda Waves from the Cross-Correlation Function in a Scattering Medium Illuminated by a Randomly Homogeneous Distribution of Noise Sources on the Basis of the First-Order Born Approximation", *Geophys. J. Int.,* **180**, 759-764 Doi: 10.1111/J.1365-246X.2009.04432.X.

Satoh, T., H. Kawase, And S. Matsushima [2001], "Differences between Site Characteristics Obtained from Microtremors, S-Waves, P-Waves, and Codas", *Bull. Seism. Soc. Am.*, **91**, 313–334.

Wapenaar, K. [2004], "Retrieving the Elastodynamic Green's Function of an Arbitrary Inhomogeneous Medium by Cross Correlation", *Phys. Rev. Lett.,* **93**, 254301-1-4.

Weaver, R.L., And O.I. Lobkis [2001], "On the Emergence of the Green's Function in the Correlations of a Diffuse Field", *J. Acoust. Soc. Am.,* **110**, 3011-3017.

Yokoi, T. And S. Margaryan [2008], "Consistency of the Spatial Autocorrelation Method with Seismic Interferometry and Its Consequence", *Geophys. Prospecting,* **56**, 435–451.